EXPERIMENTAL INVESTIGATIONS OF THE SEPARATION BEHAVIOR IN 3D SHOCK WAVE/TURBULENT BOUNDARY-LAYER INTERACTIONS

Hua-Shu Dou, Xue-Ying Deng
Institute of Fluid Mechanics
Beijing University of Aeronautics and Astronautics
Beijing 100083, P.R.China

Abstract

An experimental study has been carried out in detail for 3D shock wave / turbulent boundary-layer interactions generated by swept compression corners. The surface pressure distributions in the interaction flow field were measured at Mach numbers 2.04 and 2.50 and were compared with the oil streak patterns.Then, the separation behavior versus various parameters in 3D shock wave / turbulent boundary-layer interaction at swept compression corners was investigated and the separation mechanism of 3D interactions was analyzed. It is discovered that the separation behavior and its physical mechanism in 3D interactions are much different from 2D interactions and vary with various parameters. The separation behaviors generated by 2D ramp and by sharp fin could be connected through a serious of swept compression corner models with different sweepback angles.

Nomenclature

$L_i =$ length along corner from model apex required for the inception of cylindrical or conical flow (see Fig.7)

$L_M =$ length of upstream influence from the corner (see Fig.7)

$L_S =$ length of upstream separation from the corner (see Fig.7)

$M_\infty =$ incoming freestream Mach number

$p =$ surface static pressure

$p_s / p_\infty =$ pressure ratio at separation line

$(p_2 / p_1)_i =$ inviscid pressure rise for incipient separation

$(\nabla p) =$ pressure gradient generated by inviscid shock

$(\nabla p)_X =$ component of pressure gradient in X direction

$(\nabla p)_Z =$ component of pressure gradient in Z direction

$X =$ streamwise distance coordinate

$Y =$ vertical distance coordinate normal to the flow

$Z =$ spanwise (horizontal) distance coordinate normal to the flow

$\alpha =$ compression corner angle measured in the streamwise direction; fin angle of attack

$\beta_0 =$ angle of inviscid shock wave trace on the test surface measured from X axis (see Fig.14)

$\delta =$ incoming boundary-layer thickness

$\varepsilon =$ shock detachment angle (see Fig.15)

$\lambda =$ shock generator sweepback angle

$\lambda_{SW} =$ $90°-\beta_0$, swept angle of inviscid shock wave

on the test flat plate (see Fig.15)

$\mu =$ Mach angle

Subscripts

$A =$ apex of models

$C =$ corner line at the leading edge of models

$i =$ incipient separation

$M =$ Maximum upstream influence line

$R =$ reattachment line

$Row =$ ordinal notation of pressure taps on the flat plate

$Run =$ ordinal number of test times

$S =$ separation line

$SW =$ shock wave

$\infty =$ incoming freestream condition

I. Introduction

Three-dimensional shock wave / turbulent boundary-layer interactions are an important subject in fluid dynamics, considering both their practical significance in supersonic aerodynamics and their current standing as a pacing problem for computational fluid mechanics. Some recent reviews[1-4]illustrate that progress has been made in understanding these interactions through experimental, analytical, and computational studies. Because of the complexity of the problem and the difficulty in research, this problem is far from resolution. Among many questions raised in this research, the behavior and the physical mechanism of the interaction flow field remain poorly understood. Therefore, it is necessary to carried out further experimental work for seeking insight on this classical problem of aerodynamics.

The interaction of shock wave with a turbulent boundary-layer can result in flow separation under certain conditions. The flow separation in turn causes the change of the flow structure and the behavior of flow field. Therefore, a primary problem which was studied by many authors is to judge the incipient separation and to investigate the behavior of flow field. In the past years, the studies in separation behavior generated by shock wave / turbulent boundary-layer interactions are mostly concentrated on 2D separations, poorly on 3D separations [1-5]. Practically, the latter is the most common cases in flying vehicles and fluid machinery. In this paper the authors will study the separation behavior in 3D shock wave / turbulent boundary-layer interactions by experimental method. The surface pressure distributions in the flow field of interactions at swept compression corners

were measured at two Mach numbers, and were compared with the surface oil streak patterns. The separation behavior and the physical mechanism of interactions were exploratored. Some new viewpoints were proposed.

II. Description of Experiments

Wind Tunnel and Models

The experiments were carried out in the BUAA G-3 supersonic blowdown wind tunnel with test section $54.8 \times 47 cm^2$. A flat plate was horizontally mounted in the tunnel test section, which was used to generate a turbulent boundary layer. The swept compression corner models were mounted on the flat plate, as shown in Fig.1.A parametric set of 15 compression corner models was tested covering the ranges of sweepback angle $0° < \lambda < 60°$ and streamwise corner angle $10° < \alpha < 30°$. All the models were so mounted that the distance between the leading edge of the flat plate and the middle point of model leading edge is 590mm.

Test conditions

The test Mach numbers were 2.04 and 2.50 and Reynolds number was about 2.42×10^7 / m for both Mach numbers. The boundary layer on the plate was trippled by sand band with 3mm−width at 5mm from the plate leading edge.An approximately adiabatic 2D turbulent boundary layer was developed on the testing plate. The freestream boundary layer thickness δ, was about 0.92 cm at the middle point of leading edge of models, which was taken as a reference point, for both Mach numbers.

Measurement Technique

The measurement techniques used in the study are the surface pressure measurement and the surface flow visualization obtained from a specific kerosene lampblack streak technique as reference[6].The surface pressure measurements were performed with nine scanivalves, which were connected to 398 pressure taps(6 rows) on the flat plate. HP1000 / A700 computer and HP2250 measurement and control processor were used to gather and to process the data.

The determination of the upstream influence length from pressure distribution follows the method in Ref.6. The upstream influence length obtained from surface pressure distribution for 15 models at both Mach numbers coincides with those determined from surface streak pattern. The position of separation line was obtained from oil streak pattern. The detail of the experiments was described in reference[7].

III. Results and Discussion

Measurement Results of Surface Pressure Distribution

The surface pressure distributions of flowfields in shock wave / turbulent boundary−layer interactions generated by a set of 2D and swept compression corner models of varing parameters were measured at upstream Mach numbers 2.04 and 2.50 by using of the method described above.The typical measurement results is shown in Fig.3−6. Most of the measurement results are not presented here because of the space limit.

The behavior of the upstream influence region has been studied in Ref. 7−9. The results indicate that the upstream influence shows two type of regimes, cylindrical or conical symmetry regimes, depending upon M_∞, λ and α, as shown in Fig.7. When M_∞ is given ,there exists a boundary of cylindrical / conical regime with the variation of λ and α. When M_∞ increases, the cylindrical / conical boundary migrates toward the conical regime.

Fig.4 is the effects of model sweepback angle on the surface pressure distribution for the fixed model streamwise angle α and upstream Mach number M_∞. The vertical short lines at the X axis in the figure show the position of separation.(a) For $\alpha = 10°$, the pressure rise at the corner line is small and the upstream influence is short because of the weak shock strength. When $\lambda < 20°$, the effect of model sweepback is small and the pressure distribution has not much difference from 2D case. When $\lambda > 20°$, the pressure distribution obviously differs from 2D case. The pressure gradient in the interaction region becomes small and the upstream influence distance becomes large with λ angle increasing. (b) For $\alpha = 15°$, the pressure rise at the corner line and the upstream influence of interactions are both larger than that for $\alpha = 10°$. The effect of model sweepback becomes weak with the increasing of streamwise corner angle α. (c) For $\alpha = 24°$, the pressure distribution shape varies with the λ increasing due to the high shock strength and the change in flow structure. When $\lambda > 40°$, a peak and a valley appears respectively in the front part and in the rear part of the pressure distributions.

Fig.5 is the effect of streamwise corner angle on the pressure distribution for the given λ and M_∞. It can be seen that the pressure level at model corner line increases with the increasing of α. When α increases, the pressure distributions in front of the separation point have similar pressure gradient. The pressure ratio p_s / p_∞ at separation line almost does not change with the increasing of α. When the streamwise corner angle is large, a peak and a valley appears in the pressure distribution.

Fig.6 is the effect of M_∞ on the pressure distribution of interaction region when λ and α are fixed. The primary feature is that the increasing of M_∞ makes the pressure rise at corner line high, the pressure distribution at front of separation line steep, and the upstream influence distance short and the pressure ratio p_s / p_∞ at sparation line increases with M_∞ increasing. It can be seen that for both Mach number the peak and the valley in pressure distribution appear only for models with large λ and large α angles, i.e., for the conical region. We found by examining many data in references that the interactions generated by sharp fins also produces this kind of pressure distribution.

The separation Behavior in 3D Interactions

The upstream separation length versus model

sweepback angle λ and streamwise corner angle α is shown in Fig.8, which is gained from oil streak patterns.It should be noticed here that the α value obtained by extrapolating L_s / δ to zero represents incipient separation condition for 2D case ($\lambda = 0$). However, this method is not certain to be correct for $\lambda \neq 0$ case.Only the data obtained in the cylindrical interaction region represents incipient separation. This is because the shock detached at the model leading edge in conical region and when the incipient separation occurs the separation line was not at the corner line but away by some distance.Since it is difficult to determine the position of inviscid shock wave, the reference point of L_s / δ given in Fig.8 is the corner line.

The pressure ratio at separation line obtained from the measured surface pressure distribution at the two Mach numbers are shown in Fig.9. It can be seen that p_s / p_∞ does not vary almost with the streamwise corner angle α for given M_∞ and λ, which is similar with that in 2D interactions. Nevertheless, another parameter, λ, is introduced here. In 2D interactions, the pressure ratio at separation line for a fixed M_∞ is an invariant regardless of the generator geometry[10–11]. The data in Fig.9 is depicted in Fig.10 with another manner. Some sharp fin interaction data are also attached in the figure, where λ is taken the swept angle of inviscid shock wave. Here we assume that the shock detachment angle ε is very small compared with λ angle for the tested swept compression corner models.It can be seen that p_s / p_∞ increases with M_∞ increasing for 2D interactions ($\lambda = 0$). When λ increases from zero, p_s / p_∞ increases with M_∞ increasing in a reduced rate with respect to 2D case. For a given M_∞,p / p_∞ decreases with λ increasing in the small λ range and is an approximate constant in the large λ range. We can see that p_s / p_∞ is about 1.60 for $\lambda = 40°$ and $\lambda = 60°$ at $M_\infty = 2.04$, and is about 1.60 for $\lambda = 60°$ at $M_\infty = 2.50$.The separation pressure ratio p_s / p_∞ induced by sharp fin in this λ range is also about 1.60. This phenomena is explained as follows: These data for separation in Fig.10 is obtained for $\alpha > 15°$. The interaction of $\alpha > 15°$ for $\lambda = 40°$ and $60°$ indicates conical regimes in large λ and large α ranges.We know from above that the pressure distributions at swept compression corner interactions have same shape and features as that at sharp fin interactions in large λ range. Therefore, we can expect that the separation behavior is similar for these two type of models in the same range of λ_{sw} angle.We examined a number set of data of sharp fin interactions and found that the pressure ratio p_s / p_∞ at separation line is about 1.50–1.60 regardless of the Mach number M_∞ in the available test range of shock sweepback angle.[12–15]Therefore, we can expect that p_s / p_∞ is about 1.60 and is independent of M_∞ for the interactions generated by swept compression corner at large λ angle.

Deng and Liao have demonstrated that the separation behavior is similar for the interactions generated by sharp fin and semicone in the conical regime[16]. The behav-

iors at separation line and the incipient separation only depends upon the shock strength. The incipient separation pressure ratio is about 1.60 and independent of the generator. Therefore, it is also reasonable to expect that the separation behavior generated by swept compression corner in the conical region with large λ angle is similar with that by sharp fin.

Fig.11 is another expession form of the test data in Fig.9. The dash line in the figure is presumed from the soild line which indicates the experimentel data. The experimental data at sharp fin interactions are also given in the figure.We can see that in the range of large λ, the interaction data of swept compression corners approaches to that of sharp fins. The degree of nearness depends on λ and M_∞. For the lower M_∞ number, the minimum value of λ at which the two type of models induce same separation pressure ratio is large. It is interesting to realize that the separations generated by 2D ramp and by sharp fins, in such a way, is connected through a serious of swept compression corner models with different λ angles.

According to above analyzes, in the shock wave / turbulent boundary—layer interactions at swept shock wave, there is a critical value of λ for a given M_∞ and when λ exceeds this critical value the pressure ratio p_s / p_∞ at separation line is a constant about 1.60 regardless of the shape of the generators.Furthermore, for a range of M_∞ number, if λ angle exceeds another larger critical value, p_s / p_∞ is also independent of the M_∞ number.The larger critical value of λ is determined by the maximum Mach number in this M_∞ range.

The inviscid pressure ratio for incipient separation at sharp fin interactions $(p_2 / p_1)_i$ is also given in Fig.11. This value is about 1.50–1.60 (Ref. 16–18). Thus, it is obtained for sharp fin interactions that $(p_2 / p_1)_i \approx p_s / p_\infty$ and this equation is independent of M_∞.According to above discussion, this equation is also expected to be applicable for swept compression corner interactions in the large λ range.As a results, for a given M_∞ number, $(p_2 / p_1)_i$ and p_s / p_∞ versus model λ angle is shown in Fig.12.In the range of small λ, it is considered that $(p_2 / p_1)_i$ varies continuously with λ angle.It can be seen that $(p_2 / p_1)_i \gg p_s / p_\infty$ for 2D case, the differnce between $(p_2 / p_1)_i$ and p_s / p_∞ is reduced with λ increasing. When λ angle reaches a critical value, $(p_2 / p_1)_i \approx p_s / p_\infty$.

The conditions of incipient separation for the interactions generated by swept compression corners are shown in Fig.13, which is obtained from the surface oil streak pattern. The streamwise angle α_i for incipient separation in 2D interactions increases with M_∞ increasing.For the interactions at large λ angle, for example $\lambda = 60°$, the streamwise angle α_i for incipient separation decreases with M_∞ increasing.There is an intersection point on the curve at two Mach numbers. The interpretation for this phenomenon is evident and is as following.In the small range of λ, $(p_2 / p_1)_i$ increases with M_∞ as that in 2D case[5,11]. The higher the Mach number, the larger is the α_i. In the range of large λ angle, $(p_2 / p_1)_i$ is

an invariant as that in case of sharp fin. The higher the Mach number, the smaller is the α_i angle. Therefore, it is necessary for the curve at different M_∞ to intersect.This confirms the discussion on Fig.12 once again.

The mechanism for the Separation Behavior

In 2D interactions, the separation of boundary layer is due to the role of viscous interaction generated by the incoming boundary layer with the streamwise pressure gradient. The 3D interaction generated by swept shock wave produces a lateral pressure gradient other than the streamwise pressure gradient on the boundary layer compared with 2D interaction. This lateral pressure gradient causes the profile of boundary layer skewed, and induces a secondary flow in the boundary layer. Thus, the low—energy fluid particle in the boundary layer flows towards traverse direction. The lateral pressure gradient is larger, the more severe the secondary flow. When the secondary flow is so intense that the surface limiting streamwise line is perpendicular with the direction of local pressure gradient, the incipient separation is formed. The separation is easier to occur in 3D interactions than in 2D interactions for the same strength of shock wave because of the influence of secondary flow. In other words, the strength of shock wave for 3D separation is lower than that for 2D separation. The magnitude of the lateral pressure gradient relative to the streamwise pressure gradient can be expressed by the direction of the intersection line of shock wave at the flat plate. Here λ_{sw} is used to express this direction, as is shown in Fig.14.The angle λ_{sw} is equal to zero for 2D interactions.The angle $\lambda_{sw} = 90°-\beta_0$ for sharp fin interactions.

The angle λ_{sw} is an important parameter in 3D interactions, which represents the direction of the pressure gradient exerted on the boundary layer, as shown Fig.15. The variation of separation behavior in 3D interactions from 2D interactions to sharp fin interactions may be expressed versus the λ_{sw} angle. When $\lambda_{sw} = 0$, which corresponds to 2D interaction, the primary factor influencing the separation is the viscous interaction generated by the incoming boundary layer and the streamwise pressure gradient. When λ_{sw} increases from zero and λ_{sw} is very small, the separation difference from 2D case is little because the role of secondary flow is small. With the λ_{sw} increasing, the role of secondary flow becomes gradually important and the viscous interaction similar to that in 2D interactions plays little part.When λ_{sw} increases to a some large value, the secondary flow plays very important part. Therefore, the primary cause for separation is the secondary flow resulted from the traverse pressure gradient for 3D interaction at large λ_{sw} angle.Since the lateral pressure gradient is resulted from the outer inviscid flow field, the inviscid shock wave strength becomes the control factor of separation for 3D interaction at large λ_{sw} angle.

Following the above idea, the variation of separation behavior versus λ_{sw} angle can be divided into three regions for a given mach number, as shown in Fig.16.

Region Ⅰ : The swept angle of shock wave is very small, and the effect of secondary flow is negligible. The flow field is not much different from 2D case. The variation of behavior simply attributes to the reduction of normal Mach number of shock wave.

Region Ⅱ : The swept angle of shock wave is moderate. In this region, the viscous interaction induced by streamwise pressure gradient and the secondary flow induced by lateral pressure gradient are of same importance.The separation pressure rise decreases with the λ_{sw} increasing. In this region, the effect of secondary flow and the reduction of normal Mach number must be simultanously considered.

Region Ⅲ : The swept angle of shock wave is very large. In this region, the secondary flow resulted from the lateral pressure gradient is more important than the viscous interaction generated by streamwise pressure gradient in dominating the separation behavior. The separation pressure rise is a constant which almost does not change with the variation of λ_{sw} angle. In this region the interation is mainly controlled by an inviscid role. In other words, The strength of inviscid shock wave governs the flow field.

Some early theoretical work[19-21]demonstrates that the separation pressure rise decreases with the increasing of shock wave sweepback angle, which are worse in the range of large λ_{sw} angle. According to the present investigation, some work could be done to improve these theory.

IV. Conclusions

1. The separation behavior versus various parameters in 3D shock wave / turbulent boundary—layer interactions generated by swept compression corners is studied, which includes incipient separation and separation line behavior. It is discovered that the separation behavior at swept compression corner interactions in the conical region with large model sweepback angle λ is similar with that induced by sharp fins.

In the 3D interactions at swept compression corners, there is a critical value of λ for a fixed M_∞ number and when λ exceeds this critical value the pressure ratio at separation line p_s / p_∞ is a constant about 1.60 regardless the shape of shock generator. Furthermore, for a range of M_∞ number, if λ exceeds another larger critical value, p_s / p_∞ is also independent of the M_∞ number. The larger critical value of λ is determined by the maximum Mach number in this M_∞ range. The tendency of incipient separation pressure ratio and p_s / p_∞ at separaion line versus λ are the same. For 2D interactions, $(p_2 / p_1)_i \gg p_s / p_\infty$ and for conical interactions in the range of large λ, $(p_2 / p_1)_i \approx p_s / p_\infty$.

2. The mechanism for 3D separation is of much difference from that for 2D separation. In 2D interactions, the separation is primarily controlled by viscous effects. In 3D interactions, a lateral pressure gradient attached other than the streanwise pressure gradient. This lateral pressure gradient causes the profile of boundary layer skewed, and induces a secondary flow in the boundary—layer. Un-

der the condition of same shock wave strength, the separation in 3D interactions is easier to occur than in 2D interactions owing to the secondary flow development.

3. In 3D shock wave / turbulent boundary–layer interactions, the swept angle of inviscid shock wave is an important parameter, which shows the direction of the pressure gradient exerted on the boundary–layer and indicates which is more important in the separation of 3D interactions between the viscous interaction resulted from the incoming boundary–layer with the streamwise pressure gradient and the secondary flow induced by lateral pressure gradient.

The variation of separation behavior versus shock sweep angle can be divided into three regions for a given Mach number and the separation behavior in each region is different from the others. Only in the range of large λ_{sw} angle, the separation is primarily controlled by secondary flow which is induced by lateral pressure gradient. Therefore, in this case the separation is primarily determined by shock strength, in other words, the inviscid flow governs the separation characteristic of flow fields.

References

1. Green, J.E., "Interaction Between Shock Waves and Boundary–Layer," Progress in Aerospace Sciences, Vol.11, 1970. pp.235–340.
2. Delery, J., and Marvin, J.G., "Turbulent Shock–Wave / Boundary–Layer Interactions," AGARD–AG–280, Feb. 1986.
3. Settles, G.S. and Dolling, D.S., "Swept Shock Wave / Boundary–Layer Interactions," in AIAA Progress in Astronautics and Aeronautics: Tactical Missile Aerodynamics, edited by M.Hemsch and J. Nielsen, Vol. 104, AIAA, New York, 1986, pp.297–379.
4. Settles, G.S., and Dolling, D.S., "Swept Shock / Boundary–Layer Interactions––Tutorial and Update," AIAA Paper 90–0375, Jan., 1990
5. Delery, J.M., "Shock Wave / Turbulent Boundary Layer Interactions and Its Control," Progress in Aerospace sciences, Vol.22, No.4, 1985, 209–280.
6. Settles, G.S. and Teng, H–Y., "Cylindrical and Conical Flow Regimes of Three–Dimensional Shock / Boundary–Layer Interaction," AIAA Journal, Vol. 22, Feb. 1984, pp.194–200.
7. Dou, H.S., "Experimental and Analytical Investigations of 3D Interactions Between Shock Wave and Turbulent Boundary–Layers," Ph.D. Thesis, BUAA, Beijing, Nov., 1991.
8. Deng, X.Y., et al., "Mach Number Effects on Upstream Influence in Swept Shock wave / Turbulent Boundary–Layer Interactions," Acta Aeronautica et Astronautica Sinica, Vol.11, No.3, 1990, 127–131
9. Dou Huashu; Deng Xueying, "Measurements of the Surface Pressure Distribution in Swept Shock Wave / Turbulent Boundary–Layer Interactions," Presented at the 1st International Experimental Fluid Mechanics Congress, June, 1991, Chengdu, China.
10. Chapman, D.R., Kuehn, D.M., and Larson, H.K., "Investigation of Separated Flows in Subsonic and Supersonic Streams with Emphasis on the Effects of Transition," NACA Rept. 1356, 1958.
11. Mager, A., "Transformation of the Compressible Turbulent Boundary Layer," JAS, Vol.25, May, 1958, 305–311.
12. Tran, T.T., Tan D.K., and Bogdonoff, S.M., "Surface Pressure Fluctuations in a Three–Dimensional Shock Wave Turbulent Boundary Layer Interaction at Various Shock Strengths," AIAA Paper 85–1562, July, 1985.
13. Kim, K.S., and Settles, G.S., "Skin Friction Measurements by Laser Interferometry in Swept Shock / Boundary–Layer Interactions," AIAA Journal, Vol. 28, No.1, 1990, 133–139.
14. Oskam, B., Vas, I.E., and Bogdonoff, S.M., "Mach 3 Oblique Shock Wave / Turbulent Boundary Layer Interactions in Three Dimensions," AIAA Paper 76–336, July, 1976.
15. Wang, Y., "Investigation of Shock / Turbulent Boundary–Layer Interactions Induced by Sharp and Blunt Fins," M.S. Thesis, BUAA, Beijing, March, 1992.
16. Deng Xueying, Liao Jinhua, "Correlative Behaviours of Shock / Boundary Layer Interaction Induced by Sharp Fin and Semicone," AIAA Paper 91–1756, June, 1991
17. Korkegi, R.H., "Comparison of Shock Induced Two–and Three–Dimensional Incipient Turbulent Separation," AIAA Journal, Vol.13, April 1975, pp.534–535.
18. Zheltovodov, A.A., Maksimov, A. I. and Shilein, E., K., "Development of Turbulent Separated Flows in the Vicinity of Swept Shock Waves," The Interactions of Complex 3–D Flows, edited by Kharitonov, A.M., Akademia Nauk USSR, Inst. Theor. and Applied Mechanics, Novosibirsk, 1987, pp.67–91.
19. Myring, D.F., "The Effect of Sweep on Conditions at Separation in Turbulent Boundary– Layer / Shock–Wave Interaction," Aeronautical Quarterly, Vol. 28, May 1977, pp. 111–122.
20. Korkegi, R.H., "A Lower Bound for Three–Dimensional Turbulent Separation in Supersonic Flow," AIAA Jouranal, Vol. 23, March 1985. pp.475–476.
21. Inger, G.R., "Incipient Separation and Similitude Properties of Swept Shock / Turbulent boundary Layer Interactions," AIAA Paper 86–0345, Jan. 1986.

α \ λ	0 °	20 °	30 °	40 °	60 °
10 °	✓	✓		✓	✓
15 °	✓	✓	✓	✓	✓
20 °		✓			
24 °	✓	✓		✓	✓
30 °					✓

Table 1. Geometrical parameters of swept compression corner models
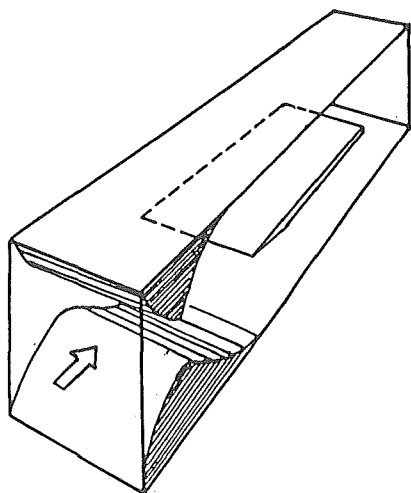
(a)
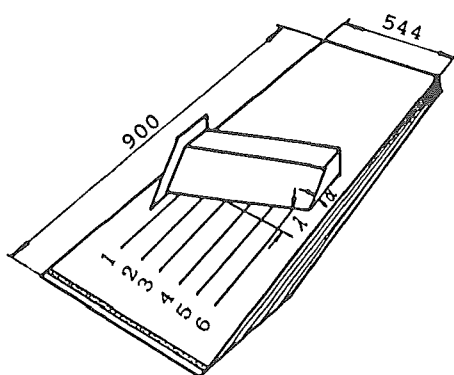
(b)

Figure 1. Diagram of experimental configuration
   (a) BUAA G–3 supersonic wind tunnel
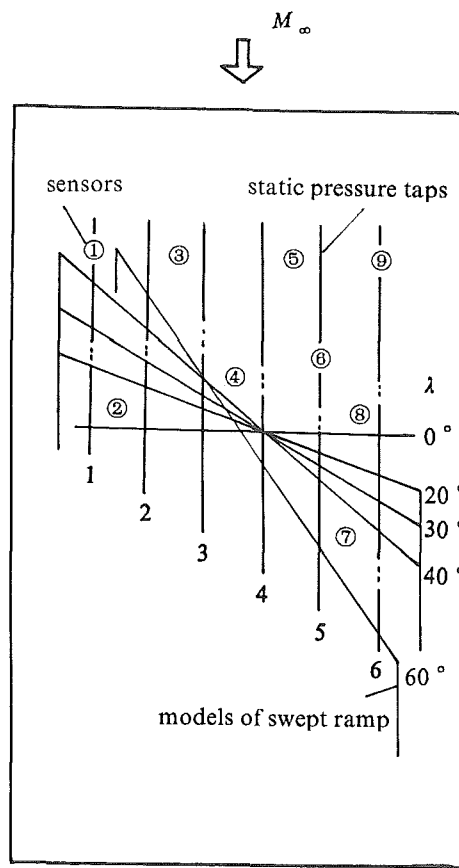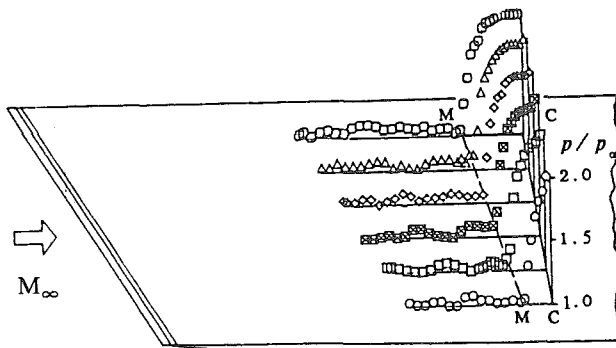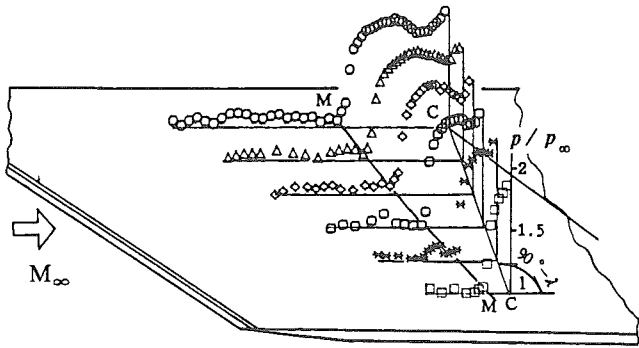   (b) Flat plate test model with swept corner

Figure 2. Schematic arangement of sensors, pressure taps and shock generators on the test flat plate

Run = 55 $M_\infty = 2.04$, $\lambda / \alpha = 20° / 24°$

(a)

Run = 52 M_∞=2.04, λ/α=40°/24°

Mach=2.04 Alfa=24 Row=4

△ Run=57 Labda=0
□ Run=55 Labda=20
◇ Run=52 Labda=40

p/p_∞

X(mm)

(b)

(b)

Figure 3. Typical results of measured pressure distributions
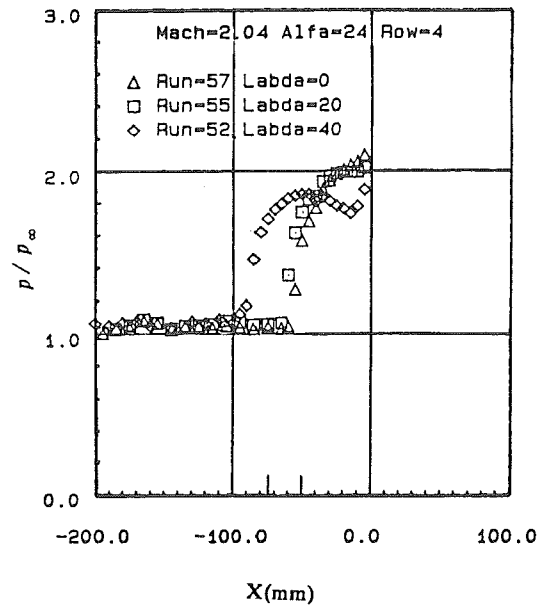
Figure 4. Effect of model sweepback angle on the pressure distributions.

Mach=2.04 Alfa=15 Row=4

△ Run=60 Labda=0
□ Run=49 Labda=20
◇ Run=54 Labda=30
○ Run=51 Labda=40

p/p_∞

X(mm)

(a)

Mach=2.04 Labda=20 Row=4

△ Run=59 Alfa=10
□ Run=49 Alfa=15
◇ Run=61 Alfa=20
○ Run=55 Alfa=24

p/p_∞

X(mm)

(a)

1549
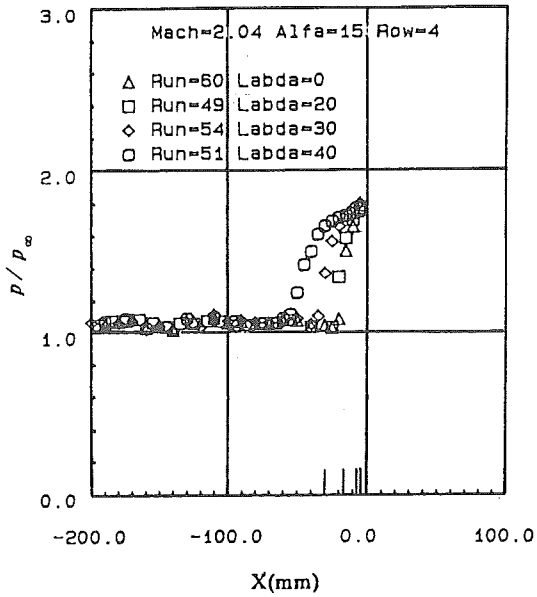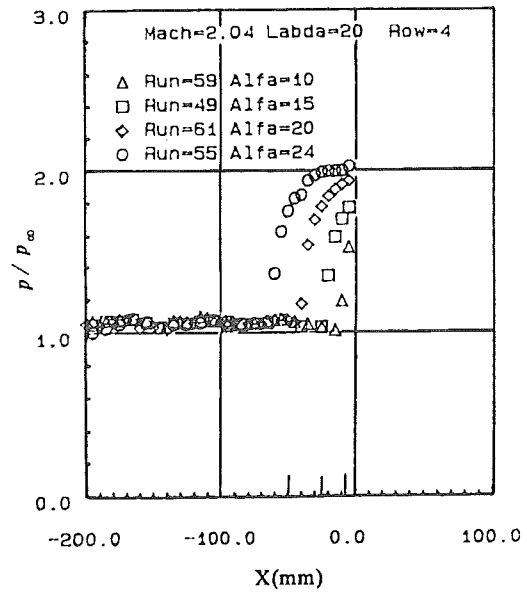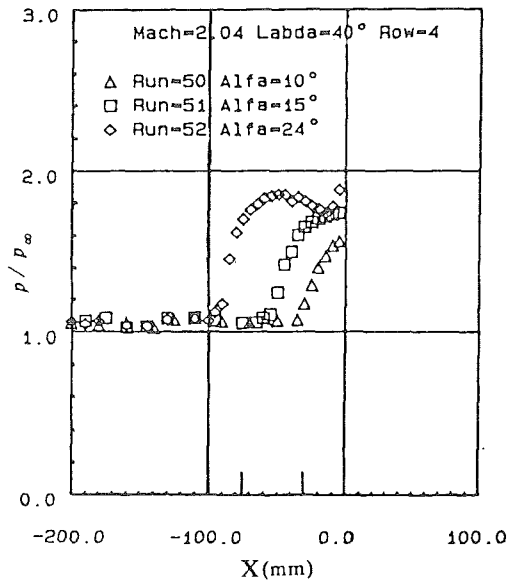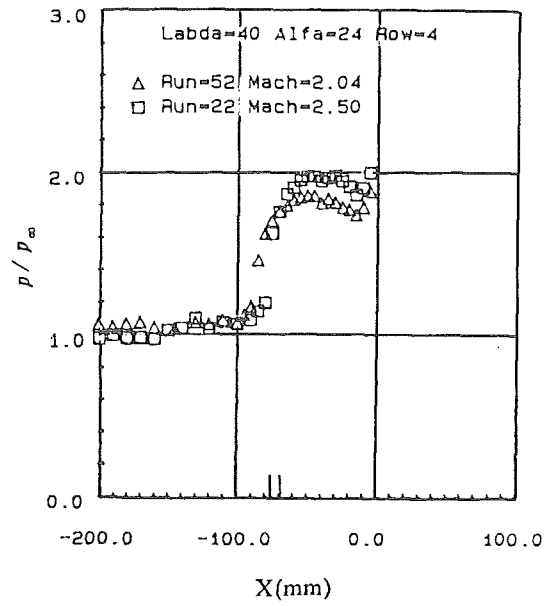
Figure 5. Effect of streamwise corner angle on the pressure distributions
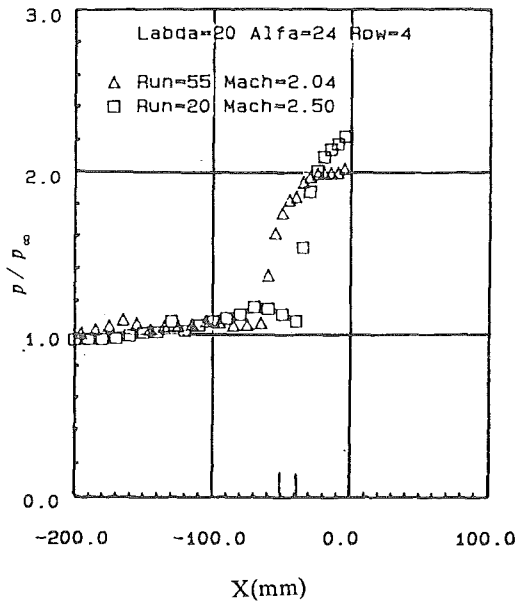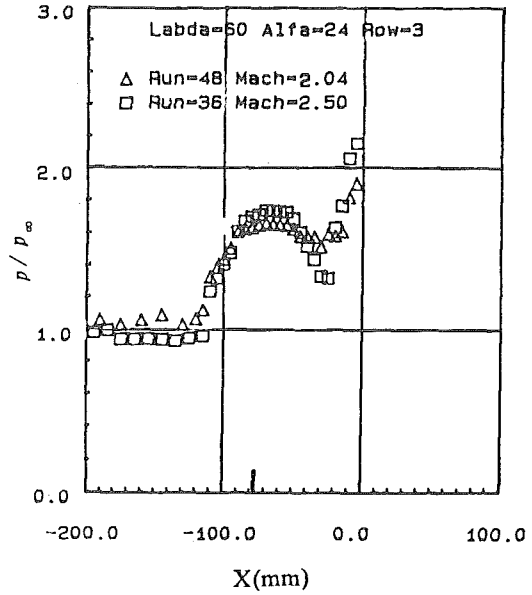
Figure 6. Effect of freestream Mach number on the pressure distributions

1550
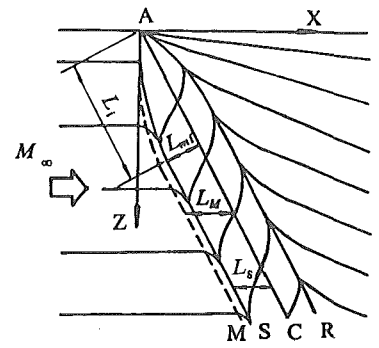
(a)Cylindrical interaction
   flowfield
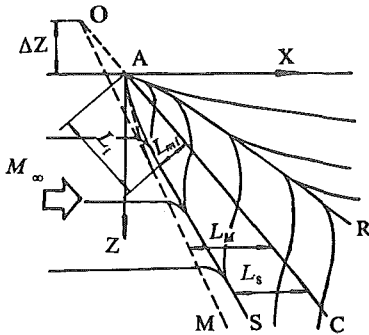
(b)Conical interaction
   flowfield
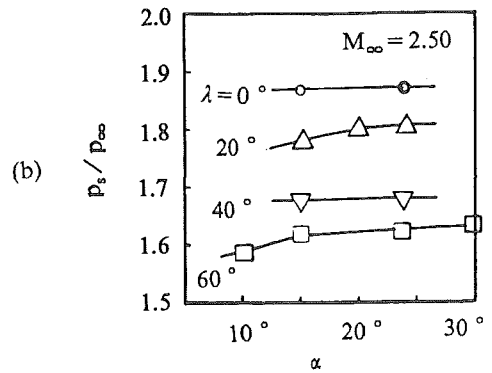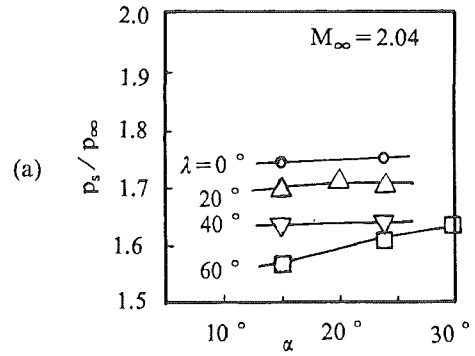
Figure 7. Schematic of surface streak pattern of swept
interaction at compression corner

Figure 9. The pressure ratio at separation line versus α
angle
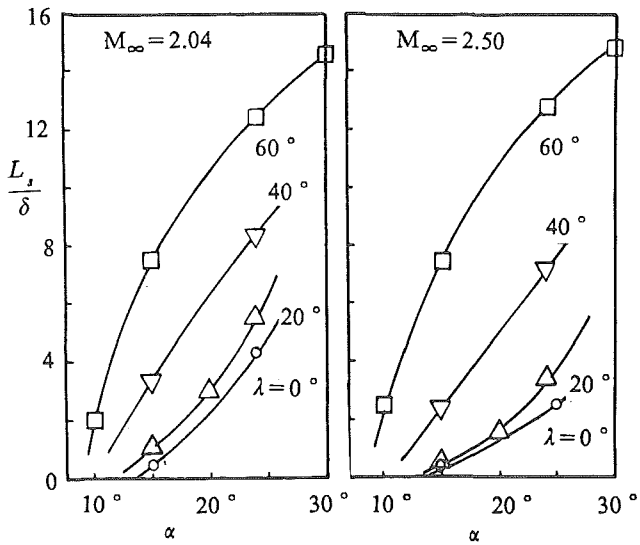
Figure 8. Upstream separation length at two Mach num-
bers (Row = 4)
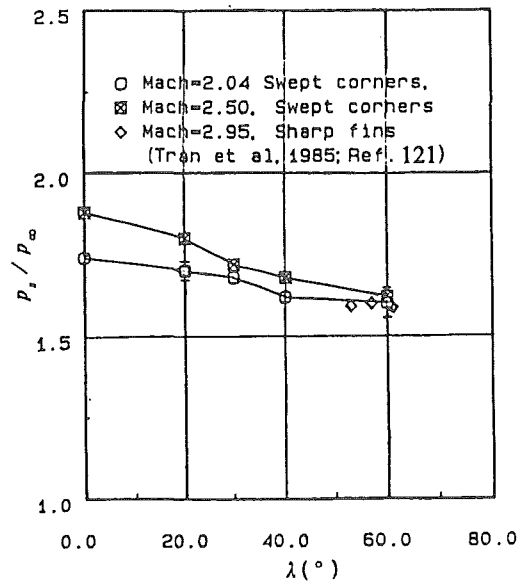
Figure 10. The pressure ratio at separation line versus λ
angle
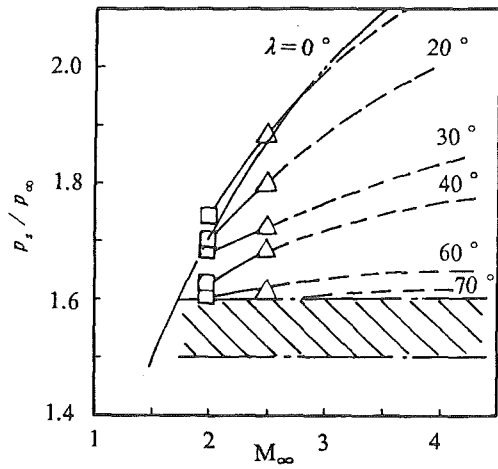
Figure 11. The pressure ratio at separation line versus Mach number

□──△ present test data

──── stretched from present test data

──··── Mager's correlation(K = 0.55) for 2D separation (see Ref.11)

\\\\\ pressure ratio at separation line for sharp fin interactions

──·── inviscid pressure rise for incipient separation at sharp fin interactions
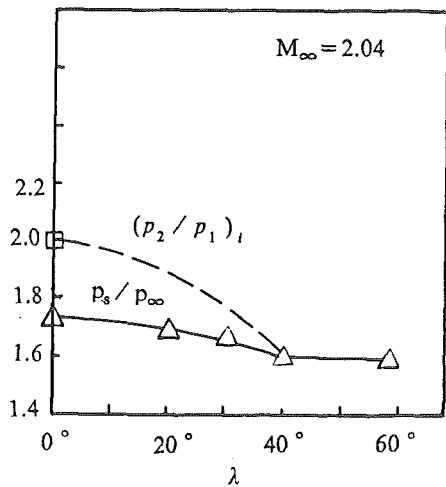
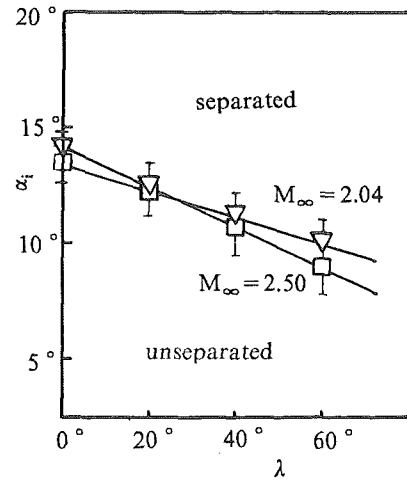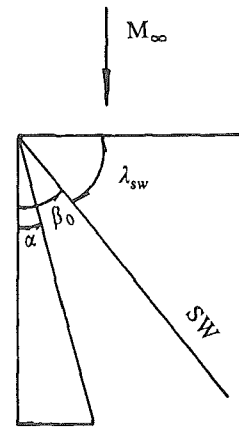Figure 12. $(p_2 / p_1)_i$ and p_s / p_∞ versus λ angle at $M_\infty = 2.04$
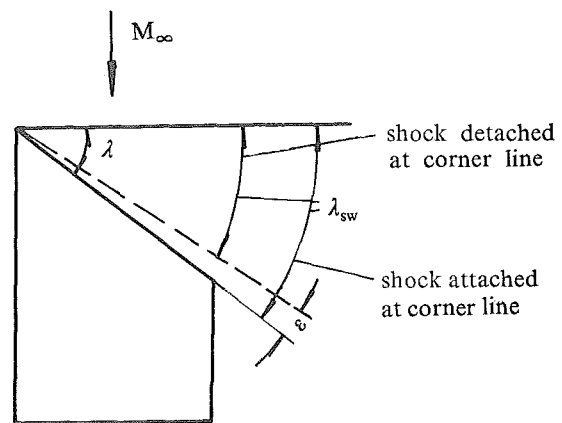

Figure 13. Variation of streamwise corner angle for incipient separation versus model sweepback angle

(a)

(b)

Figure 14. Intersection of inviscid shock wave on the test flat plate
(a) sharp fin as shock generator
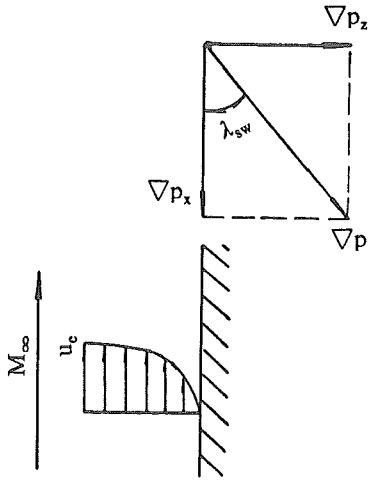(b) swept ramp as shock generator

1552

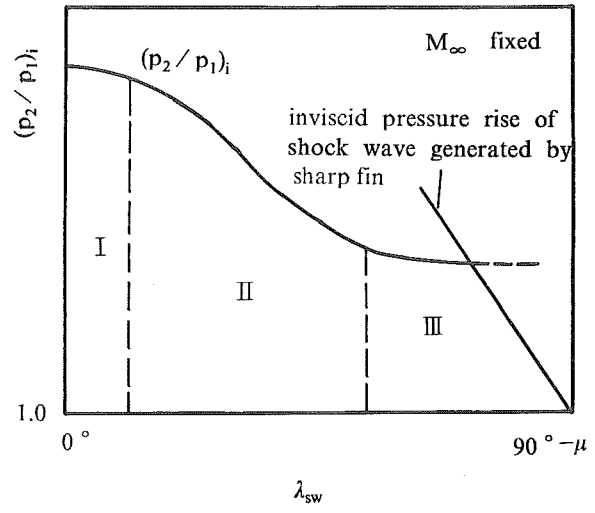Figure 15. The pressure gradient exerted on the boundary layer

Figure 16. The behavior of incipient separation in each ranges of λ_{sw}